Supporting Information

Anharmonic rattling leading ultra-low lattice thermal conductivity in $Cu_{12}Sb_4S_{13}$ tetrahedrites

Kewal Singh Rana,[a] Nidhi,[b] Chandan Bera,[b] Kanishka Biswas,[c] and Ajay Soni[a]*

[a]School of Physical Sciences, Indian Institute of Technology Mandi, Mandi 175075, Himachal Pradesh, India

[b]Institute of Nano Science and Technology, Knowledge City, Sahibzada Ajit Singh Nagar, 140306 Punjab, India

[c]New Chemistry Unit, School of Advanced Materials and International Centre of Materials Science, Jawaharlal Nehru Centre for Advanced Scientific Research (JNCASR), Jakkur, Bangalore 560064, India

Corresponding Author Email: ajay@iitmandi.ac.in

The Supporting Information includes structural, phonon dispersion relations, eigen vector visualizations, electrical, thermal and Raman spectroscopic measurements.

S1: Sound Velocity Measurement Details:

The mean sound velocity (v_m) was estimated from the longitudinal (v_l) and transverse (v_t) sound *velocities* via the formula:

$$v_m = \left(\frac{3}{v_l^{-3} + 2v_t^{-3}}\right)^{1/3} \quad \text{..... (1)}$$

The Grüneisen parameter (γ_G) was estimated using the formula:

$$\gamma_G = \frac{3}{2}\left(\frac{1+v_p}{2-3v_p}\right) \quad \text{..... (2)}$$

Where, v_p is the Poisson ratio which is calculated from v_l and v_t through:

$$v_p = \frac{1 - 2\left(\frac{v_t}{v_l}\right)^2}{2 - 2\left(\frac{v_t}{v_l}\right)^2}$$, ……. (3)

The Debye temperature (Θ_D) was calculated from the mean sound velocity (v_m) using:

$$\Theta_D = \frac{h}{k_B}\left(\frac{3N}{4\pi V_u}\right)^{1/3} v_m$$, ……. (4)

where h , N and V_u are the Planck's constant, number of atoms in a unit cell and unit-cell volume.[1]

Further, the bulk (B) and shear modulus (G) were determined using the v_l , v_t and density (ρ) of the material using the equation:

$$B = v_l^2\rho - \frac{4}{3}(v_t^2\rho)$$, ……. (5)

$$G = v_t^2\rho$$. ……. (6)

S2: Lorenz number Calculations:

The Lorenz number (L) is calculated by fitting the reduced chemical potential (η), which is derived from the temperature dependent Seebeck coefficient, single parabolic band and acoustic phonon scattering,[2] via:

$$S = \frac{k_B}{e}\left(\frac{2F_1(\eta)}{F_0(\eta)} - \eta\right)$$ ……. (8)

and

$$L = \left(\frac{k_B}{e}\right)^2 \frac{3F_0(\eta)F_2(\eta) - 4F_1^2(\eta)}{F_0^2(\eta)}$$ ……. (9)

Here, $\eta = \left(\frac{E_F}{k_B T}\right)$, in which k_B being the Boltzmann's constant and the Fermi integral, $F_n(\eta)$ is denoted by:

$$F_n(\eta) = \int_0^\infty \frac{\epsilon^n}{1 + e^{\epsilon - n}} \quad \text{..... (11)}$$

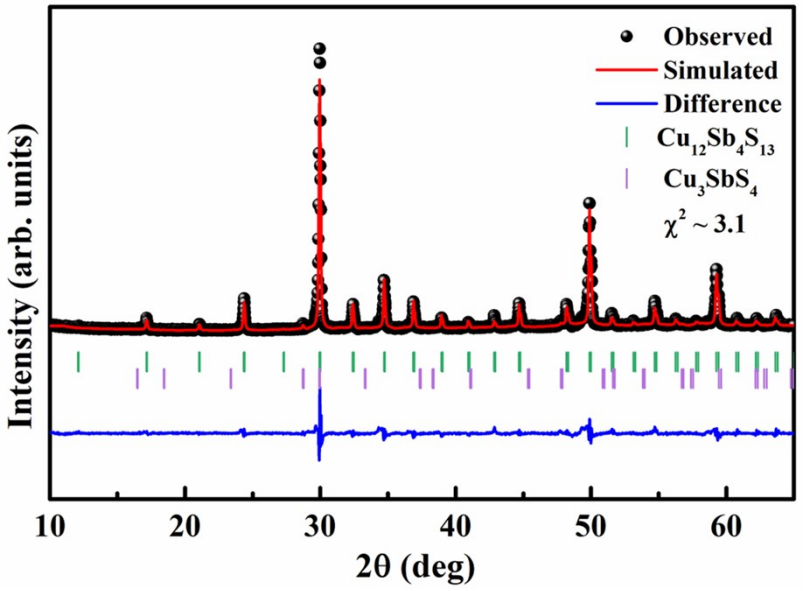

Fig. S1 Rietveld refined XRD pattern of $Cu_{12}Sb_4S_{13}$ using Fullprof Suite software.

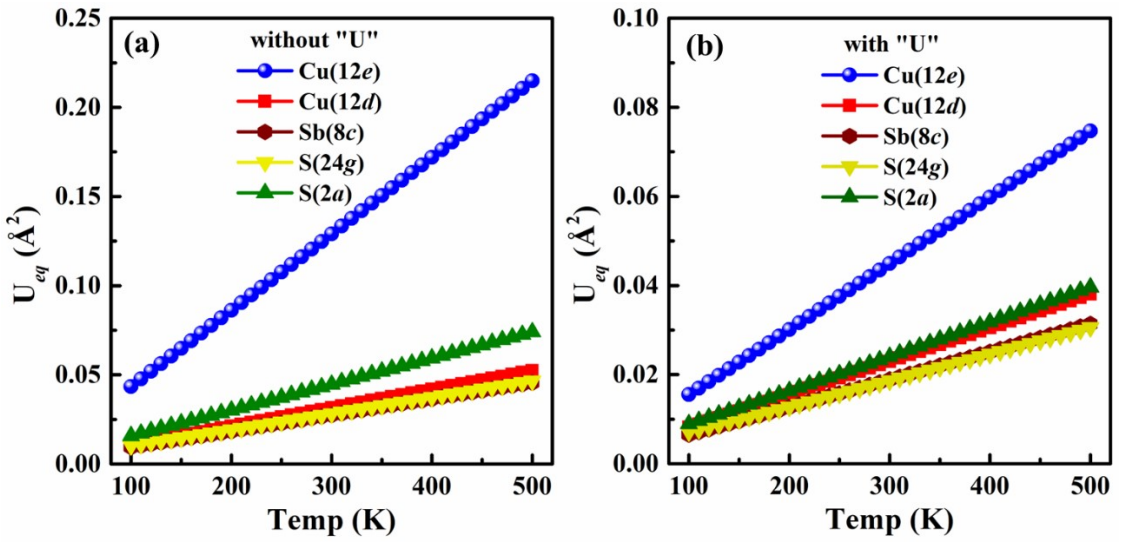

Fig. S2 The Cu(12*e*) atoms exhibit a large atomic displacement parameter (ADP: U_{eq}), with temperatures, in comparison with other atoms (Sb, S) and Cu(12*d*), for (a) without U (Coulombic interaction term) and (b) with U.

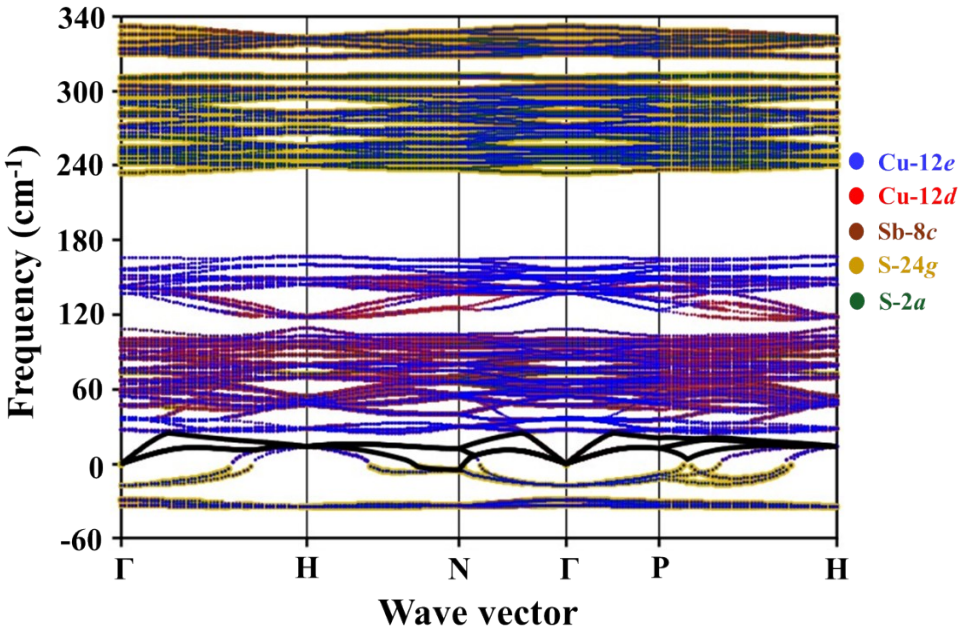

Fig. S3 The atom-projected phonon dispersion relation without *U* (Coulombic interaction term) for $Cu_{12}Sb_4S_{13}$.

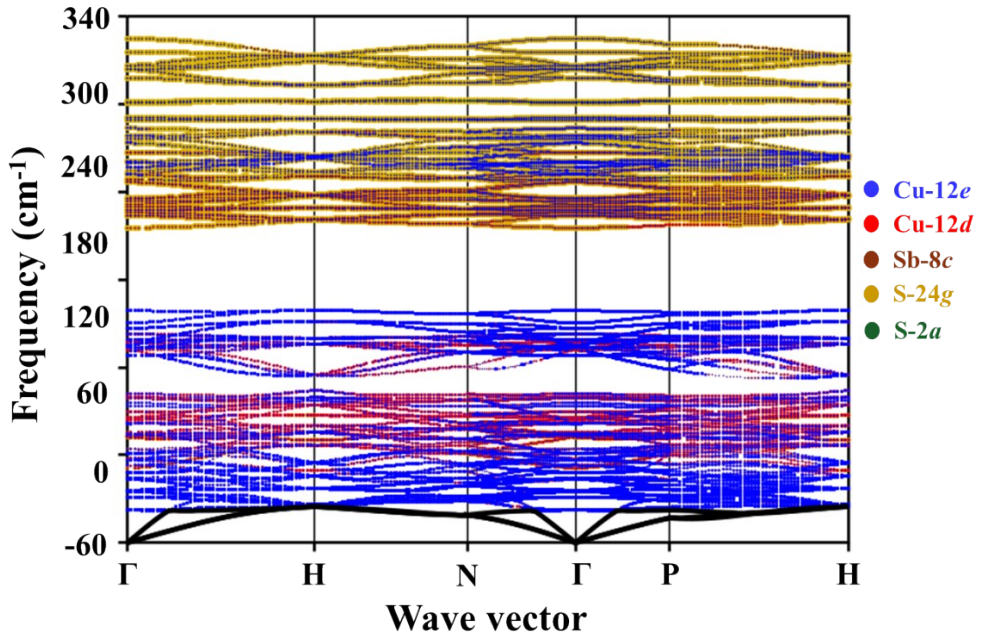

Fig. S4 The atom-projected phonon dispersion relation with *U* (Coulombic interaction term) for $Cu_{12}Sb_4S_{13}$.

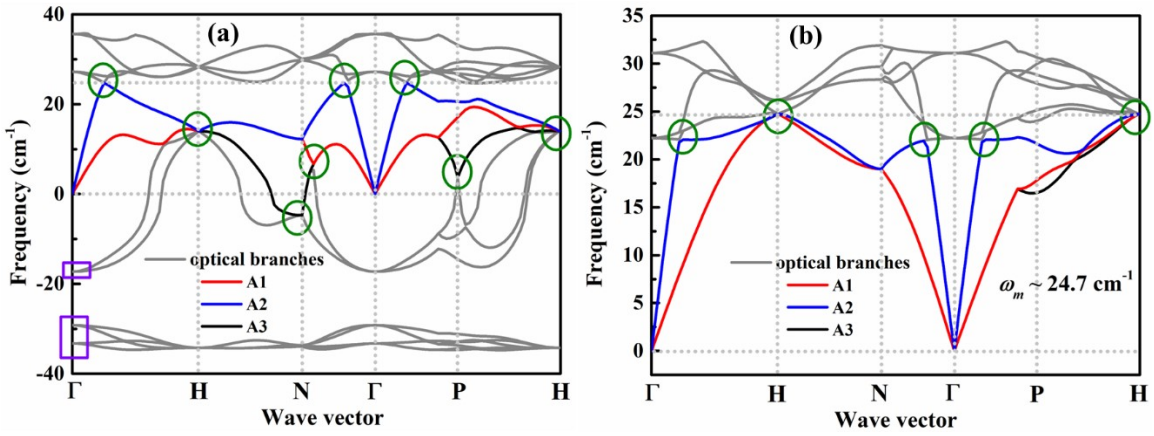

Fig. S5 The low energy acoustic and optical phonon interactions shown in green circle (a) without *U* parameter, and the purple rectangular box at *Γ*-point represents the negative modes frequencies, (b) with *U* parameter, for $Cu_{12}Sb_4S_{13}$, respectively.

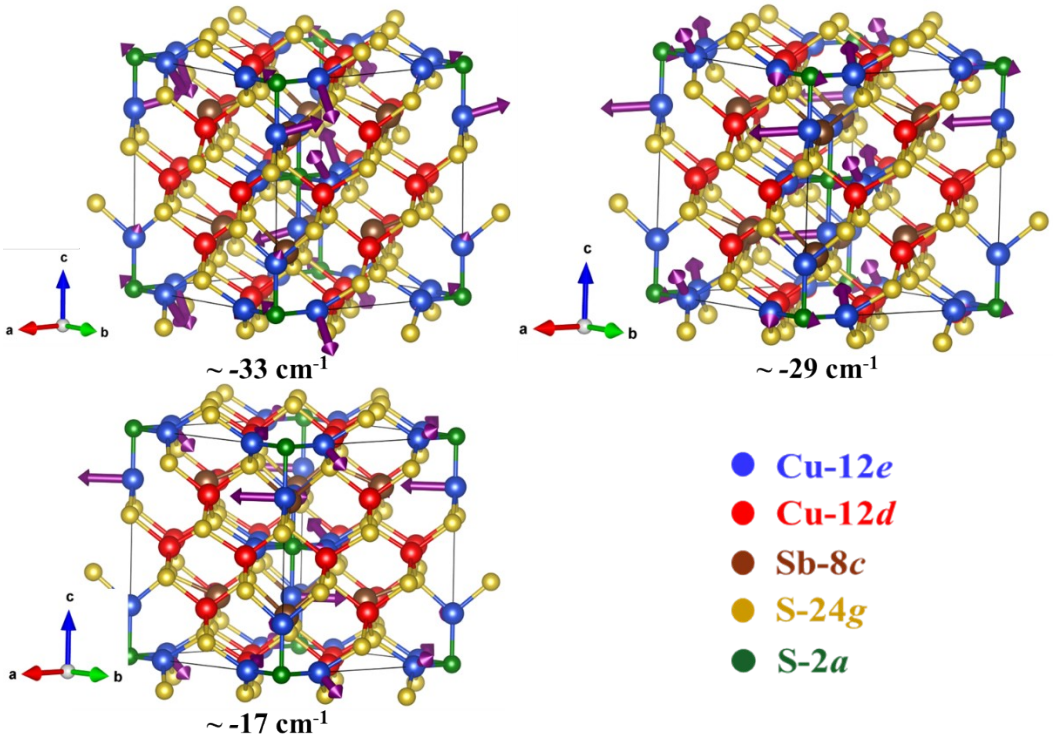

Fig. S6 The eigen vector visualization of imaginary (unstable) vibrational modes, which strongly involves the dominating Cu(12*e*) atom vibrations (shown in purple arrow).

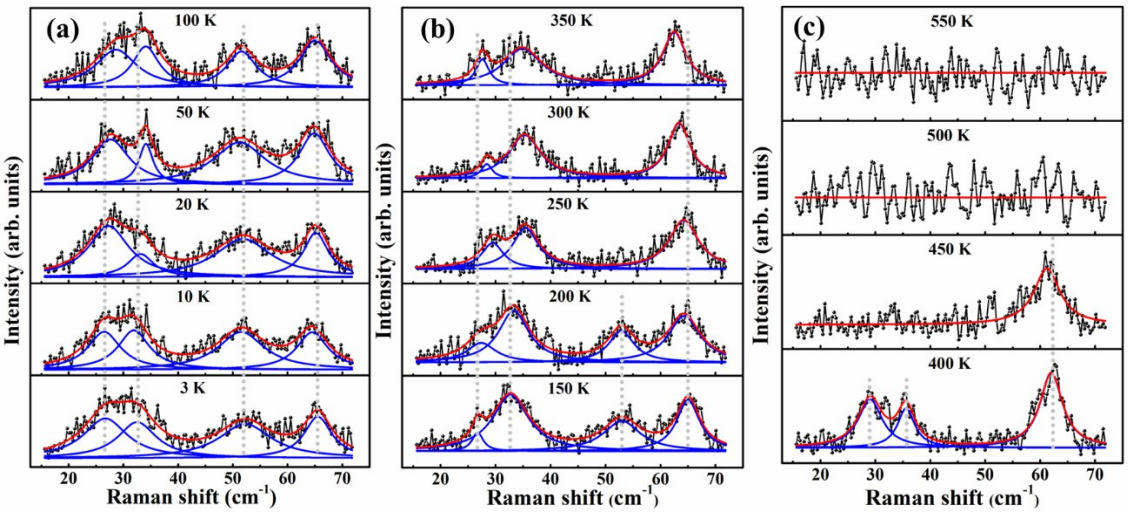

Fig. S7 Temperature dependent (a) 3-100 K, (b) 150-350 K, and (c) 400-550 K in the low-frequency (~15-75 cm^{-1}) Raman spectra fitting through Lorentzian function.

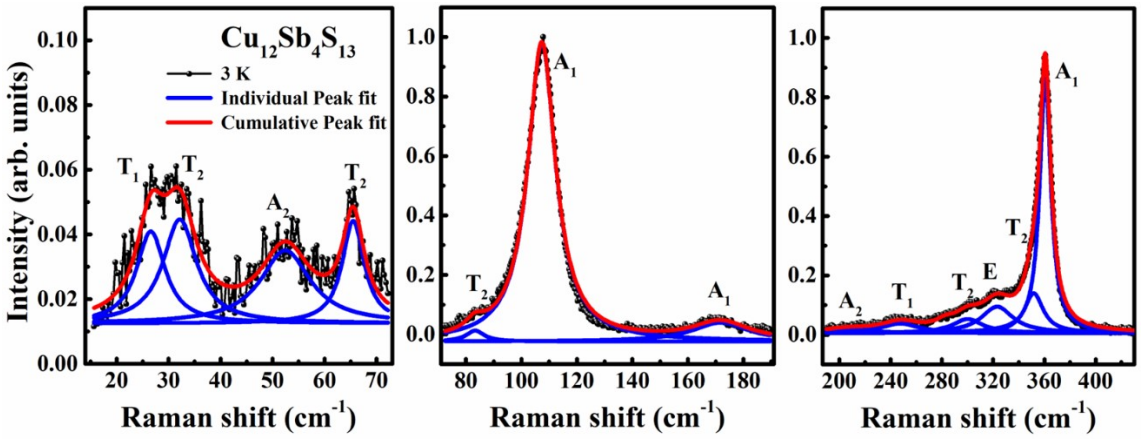

Fig. S8 Lorentzian function fitting of Raman active mode at 3 K, where the low frequency modes are clearly visible for $Cu_{12}Sb_4S_{13}$.

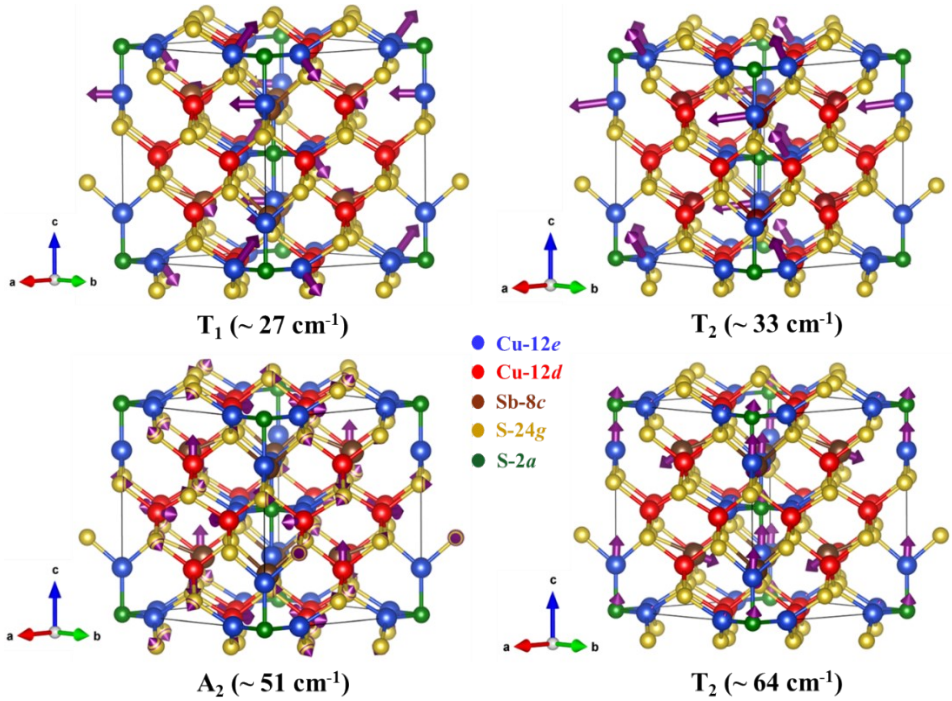

Fig. S9 The eigen vector visualization for low-frequency Raman active modes, which strongly involves the dominating vibrations of Cu(12*e*) atoms.

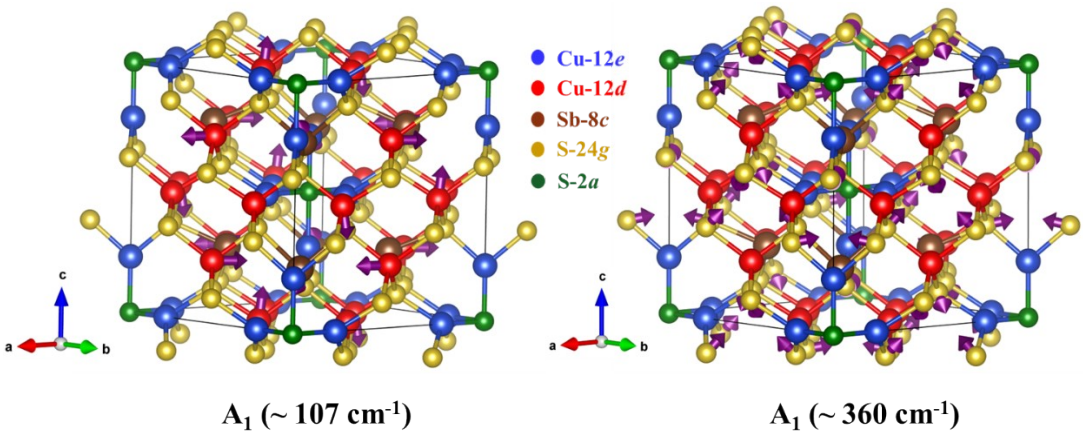

Fig. S10 The eigen vector visualization of highest intensive Raman active modes, which involves the dominating vibrations of Cu(12*d*), Sb(8*c*) and S(24*g*) atoms.

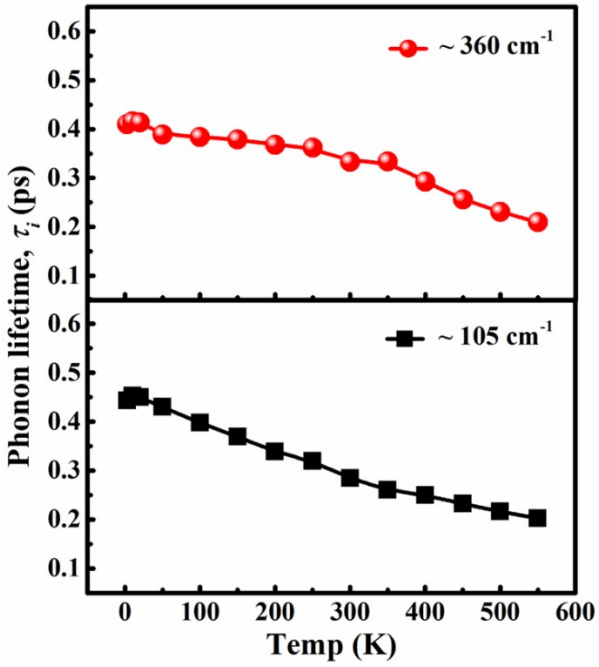

Fig. S11 Temperature dependent (3 – 550 K) phonon lifetime (τ_i) of prominent vibrational mode of $Cu_{12}Sb_4S_{13}$.

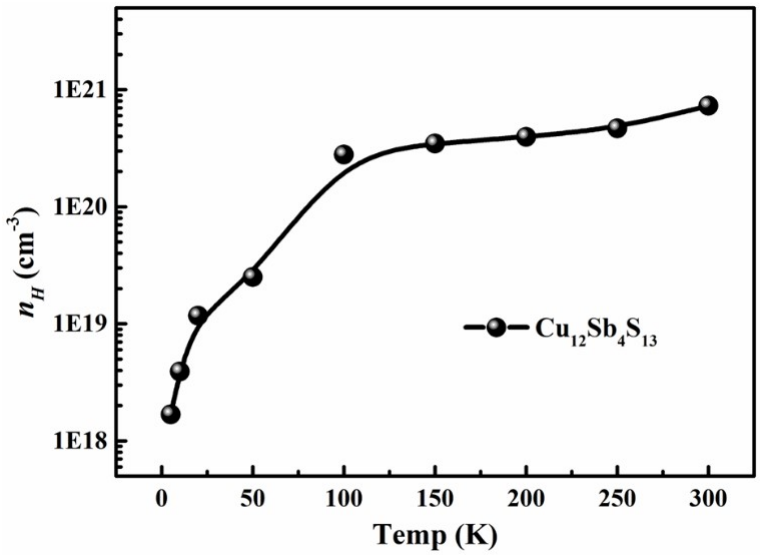

Fig. S12 The temperature dependent carrier concentration (^{n_H}), plot for $Cu_{12}Sb_4S_{13}$.

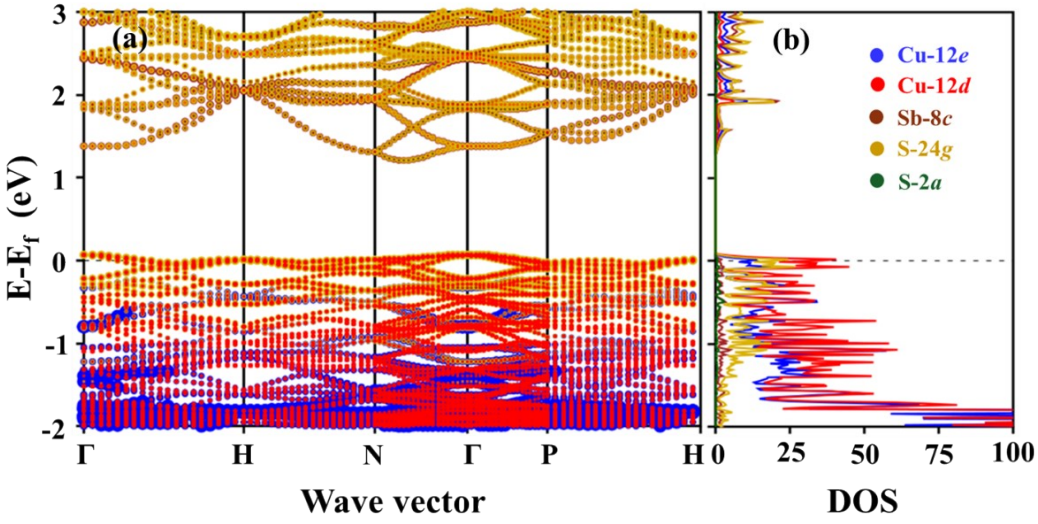

Fig. S13 The (a) electronic band structure and (b) density of states for $Cu_{12}Sb_4S_{13}$ without *U* (Columbic interaction) term.

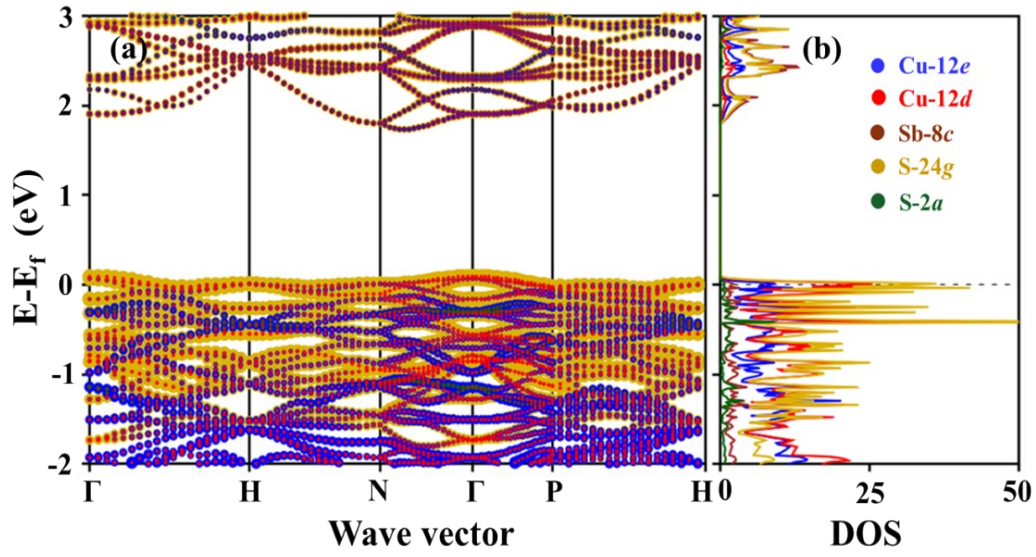

Fig. S14 The (a) electronic band structure and (b) density of states for $Cu_{12}Sb_4S_{13}$ with *U* (Columbic interaction) term.

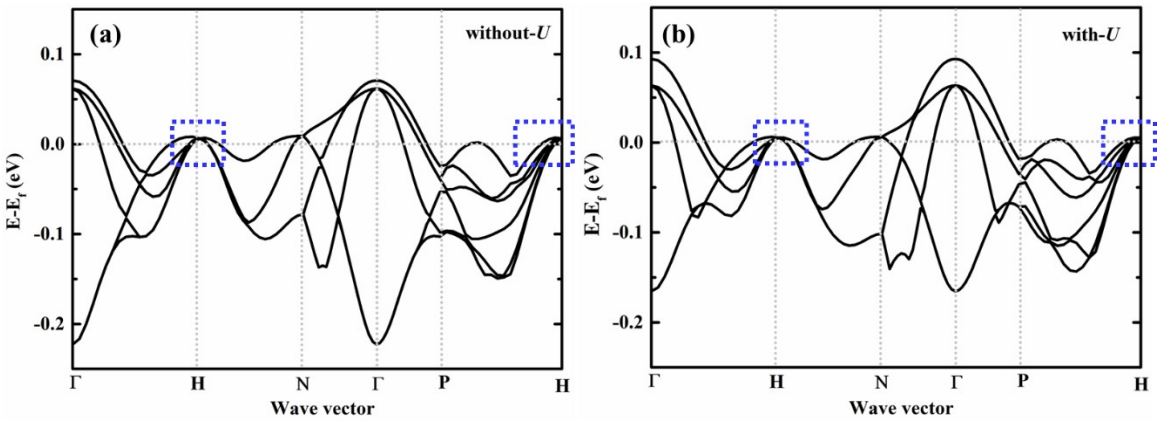

Fig. S15 The convergence of valance band near the Fermi energy (E_f) level.

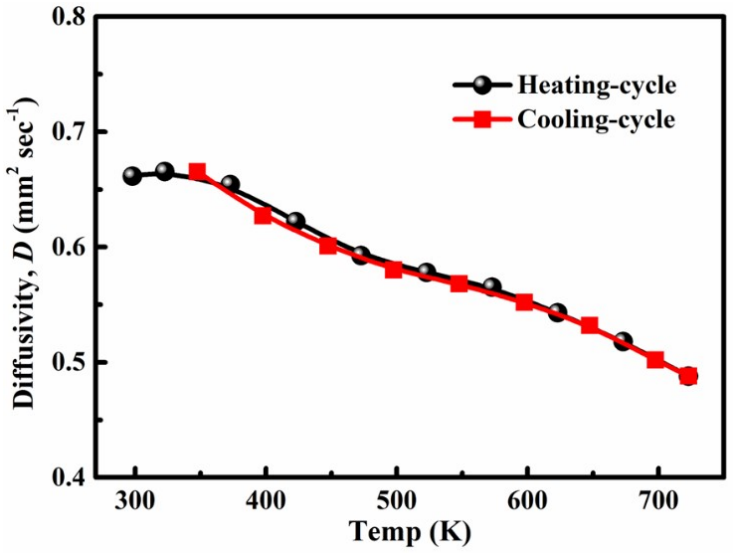

Fig. S16 Temperature dependence diffusivity (D) for $Cu_{12}Sb_4S_{13}$.

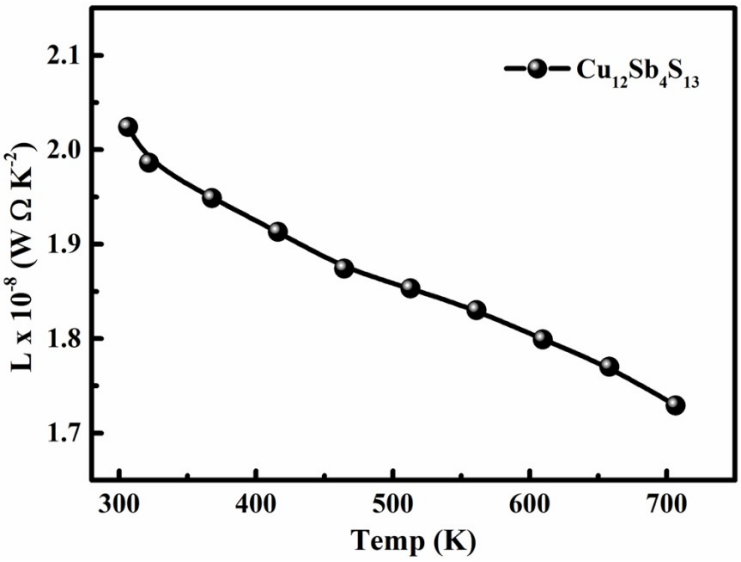

Fig. S17 The estimated Lorenz number (L) for $Cu_{12}Sb_4S_{13}$.

Table S1. The Rietveld refined crystal structure parameters for $Cu_{12}Sb_4S_{13}$.

a = b = c (Å)	**Cu(12*e*)**	**Cu(12*d*)**	**Sb(8*c*)**	**S(2*a*)**	**S(24*g*)**	**V(Å^3)**

10.3318	x = 0.25 y = 0.50 z = 0.00	x = 0.2108 y = 0.00 z = 0.00	x = 0.2665 y = 0.2665 z = 0.2665	x = 0.00 y = 0.00 z = 0.00	x = 0.1111 y = 0.1111 z = 0.3642	1102.89

Table S2. The fitting parameters obtained from the heat capacity (1*D*-3*E* model) data.

Fitting parameters (1*D*-3*E*) model	**$Cu_{12}Sb_4S_{13}$**
γ (J mol^{-1} K^{-2})	~ 0.085 ± 0.005
β (J mol^{-1} K^{-4})	~ 4.28E-4 ± 1.9E-5
A (J mol^{-1} K^{-1})	~ 11.3 ± 0.4
Θ_{E1} (K)	~ 24.7 ± 0.3
B (J mol^{-1} K^{-1})	~ 98.0 ± 3.5
Θ_{E2} (K)	~ 64.3 ± 0.8
C (J mol^{-1} K^{-1})	~ 238.8 ± 2.5
Θ_{E3} (K)	~ 123.7 ± 1.4
R^2 (Adj. R-Square)	~0.9999
χ^2 (Reduced Chi-Square)	1.03E-4

References:

1. P. Acharyya, T. Ghosh, K. Pal, K. S. Rana, M. Dutta, D. Swain, M. Etter, A. Soni, U. V. Waghmare and K. Biswas, *Nature Communications*, 2022, **13**, 5053.
2. K. Biswas, J. He, I. D. Blum, C.-I. Wu, T. P. Hogan, D. N. Seidman, V. P. Dravid and M. G. Kanatzidis, *Nature*, 2012, **489**, 414-418.